Forensic Science International 223 (2012) 298–305

Contents lists available at SciVerse ScienceDirect

Forensic Science International

journal homepage: www.elsevier.com/locate/forsciint

Monitoring of illicit pill distribution networks using an image collection exploration framework

Jorge Camargo [a], Pierre Esseiva [b,*], Fabio González [a], Julien Wist [c], Luc Patiny [d]

[a] Universidad Nacional de Colombia, Bioingenium Research Group, Colombia
[b] Université de Lausanne, Institut de Police Scientifique, Switzerland
[c] Departamento de Química, Universidad del Valle, AA 25360, Cali, Colombia
[d] École Polytechnique de Lausanne, Institute of Chemical Sciences and Engineering, Switzerland

ARTICLE INFO

Article history:
Received 12 March 2012
Received in revised form 7 August 2012
Accepted 3 October 2012
Available online 26 October 2012

Keywords:
Drug intelligence
Image
Ecstasy (XTC)
Similarity function
Clustering and visualization

ABSTRACT

This paper proposes a novel approach for the analysis of illicit tablets based on their visual characteristics. In particular, the paper concentrates on the problem of ecstasy pill seizure profiling and monitoring. The presented method extracts the visual information from pill images and builds a representation of it, i.e. it builds a pill profile based on the pill visual appearance. Different visual features are used to build different image similarity measures, which are the basis for a pill monitoring strategy based on both discriminative and clustering models. The discriminative model permits to infer whether two pills come from the same seizure, while the clustering models groups of pills that share similar visual characteristics. The resulting clustering structure allows to perform a visual identification of the relationships between different seizures. The proposed approach was evaluated using a data set of 621 Ecstasy pill pictures. The results demonstrate that this is a feasible and cost effective method for performing pill profiling and monitoring.

1. Introduction

According to the World Drug Report 2011 published by the United Nations Office on Drugs and Crime [1] amphetamine type stimulants (ATS) represent one of the most significant drug problems worldwide with an annual prevalence ranging between 0.3% and 1.3% of the worldwide population aged 15–64 (between 13.7 and 56.4 million people). Many efforts have been undertaken during the last decade to propose new methods for highlighting the links between seizures and thereby allowing the deciphering of traffic mechanisms of criminal organizations. Illicit pill monitoring attempts to determine the origin of pills, the routes used to traffic them and the chemicals used for their production. This process implies establishing links between pills belonging to different seizures. A common assumption made by different illicit pill profiling and monitoring methods is that pills having similar physical and chemical profiles are likely connected. Indeed, large scale projects regrouping different forensic laboratories have investigated the feasibility of deploying harmonized methods for the profiling of amphetamine [2–7] or methamphetamine [8–10] by building physical and chemical profiles of pills.

New analytical developments like Solid Phase MicroExtraction (SPME) [11–14] or Isotope-Ratio Mass Spectrometry [10,15,16] (IRMS) have also been tested for bringing additional knowledge regarding the composition of the illicit drugs seizures. However, ensuring that data obtained by methods such as GC–MS or GC–IRMS are comparable is expensive and time consuming, since it requires the adoption of highly standardized processes. It is therefore important to offer alternative methods that are less expensive, easier to deploy and to maintain in the long term. For instance, the actual philosophy consists of developing databases that can be shared between several laboratories.

In turn, physical properties of ATS such as diameter, weight and thickness are readily determined in a first step and were shown useful [17]. The visual features were also showed promising at this stage [18–22]. Processes to measure these properties or to extract features may easily be performed automatically and do not require tedious and expensive standardization procedures or expensive equipment.

Therefore, this paper proposes an agile method for illicit pill profiling and monitoring that relies on the assumption that two illicit pills, which are visually similar, are likely related. In particular, the paper proposes a pill profiling method based on

* Corresponding author at: Institut de Police Scientifique, Ecole des Sciences Criminelles, Université de Lausanne, Batochime, 1015 Lausanne-Dorigny, Switzerland. Tel.: +41 21 692 46 50.
E-mail addresses: jecamargom@unal.edu.co (J. Camargo), pierre.esseiva@unil.ch (P. Esseiva), fagonzalezo@unal.edu.co (F. González), julien.wist@correounivalle.edu.co (J. Wist), luc.patiny@epfl.ch (L. Patiny).

0379-0738/$ – see front matter © 2012 Elsevier Ireland Ltd. All rights reserved.
http://dx.doi.org/10.1016/j.forsciint.2012.10.004

pill visual appearance, and a pill monitoring strategy that combines a discriminative and clustering model based on pill visual similarity functions. In general, visual similarity depends on different visual features such as color, texture and shape. This paper explores different image representations it offers two main tools for performing pill monitoring: first, a discriminative model that is able to determine whether two different pills belong to the same batch, and second, a visual exploration tool, based on a pill clustering, which shows the relationships between different pill and production batches in the pill database. Thus, we provide the users with a fast and reliable method to guide them during their inquiries, while more sophisticated and thereby more expensive methods such as gas chromatography coupled to mass spectrometry (GC–MS) or IRMS may be used only when a court requires evidence. The proposed information is initially dedicated for investigative purposes in conjunction with complementary law enforcement information like wire or informant data. We believe that is important to dissociate information for evidence purposes for the court from data dedicated for intelligence purposes for the law enforcement. Law enforcement needs to be provided with information that could be used as a triggering factor for initiating new enquiry indications or to consolidate existing information about the structure of a criminal organization. The information leaded by the fact that two pills share a similar "physical profile" is a piece of information pointing to the fact that the two pills and by extension the two seizures share enough similarities to be considered as an added value for investigators for confirming or strengthen their inquiry hypotheses. Being dedicated for law enforcement purpose argues also in favor of having access rapidly to the information as it is proposed when focusing on physical characteristics that could be extracted without any sophisticated analytical method. If one needs to move to the evidential level, then of course more complete data allowing inferring the source level have to be deployed like for example GC–MS profile extraction.

2. Methodology

2.1. Image acquisition

Images of illicit pills were acquired using a Nikon D90 camera with a 5000 K illuminant inside a digital imaging lightbox. The pills were laid on a black photo paper containing a white square of 2.5 mm side [21]. Each original image was binarized to discriminate all the objects from the background, while the background of the resulting image was corrected to black; and the largest object, i.e. the pill itself, was extracted. This process is illustrated in Fig. 1.

2.2. Feature extraction

Two main types of visual features were used to characterize the visual content of images. One based on standard visual features that globally characterize color, texture and shape. It was applied to the images acquired as described in the previous section; and the other one adapted to the particularities of this collection through the construction of a visual codebook. Both strategies are described in the following subsections (Fig. 2).

2.2.1. Standard visual features

The aim of feature extraction is to identify and extract the relevant information. For this task we follow a content-based image retrieval (CBIR) strategy, where visual patterns such as texture, color and edges were extracted to represent the image content. These features can be represented as histograms, which indicate the frequency associated with visual patterns present in the image. The following standard visual features were extracted:

- *Gray*. A histogram is built by counting the number of occurrences of each one of the 256 intensity values in a gray version of the pill image.
- *Color*. A RGB color space was used to represent pill color that is divided into 512 elements using 8 bins per color channel [23]. A 512 bins histogram ($8 \times 8 \times 8 = 512$) is built by counting the number of pixels in the image that correspond to each one of the 512 subspaces.
- *Local binary patterns*. Local binary patterns [24] are a measure of image texture. The goal is to define a set of binary patterns (black and white) that can be found around each pixel. This pattern is identified by analyzing the relative intensity of the pixel and their 8 nearest neighbors. The intensity of each pixel is compared with the intensity of its 8 neighbors. A value of 1 is assigned to the neighbors with higher intensities, while 0 otherwise. Thus, a word of 8 bits is assigned to each pixel corresponding to a value between 0 and 255.
- *Sobel edges*. The Sobel operator [25] detects image borders by calculating the derivative in one local region of the image by identifying the magnitude and change vector direction. The information codified in the histogram is related to the change in magnitude, which indicates the presence of salient or smooth edges. It is common to use a 3×3 operator to determine the changes in intensity of the neighbors and to represent these changes using a 512 bins histogram.
- *Tamura texture*. This visual feature captures texture information such as coarseness, contrast, directionality, linelikeness, regularity and roughness [26]. A 512 bins histogram is built with the space generated by the first three characteristics, as described for the color histogram.
- *Invariant feature*. This type of feature extracts texture characteristics that are invariant to different conditions such as rotation, translation and scale [23].

2.2.2. Non-standard features: bag of visual features

The bag of features (BoF) [27] approach is another manner to represent the content of an image. The BoF representation is inspired by the human visual system, since it perceives an object by integrating its constituent components, referred to as patches

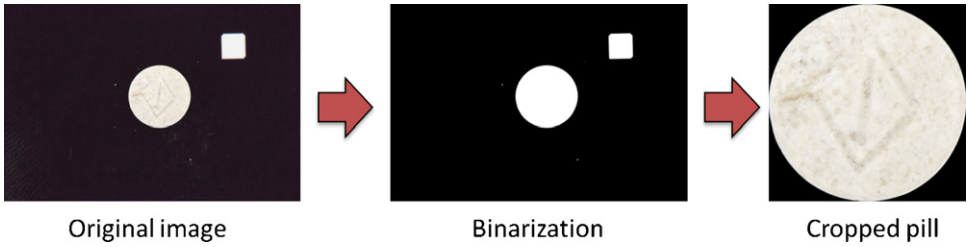

Fig. 1. Diagram that illustrates the pre-processing applied to the original pill pictures.

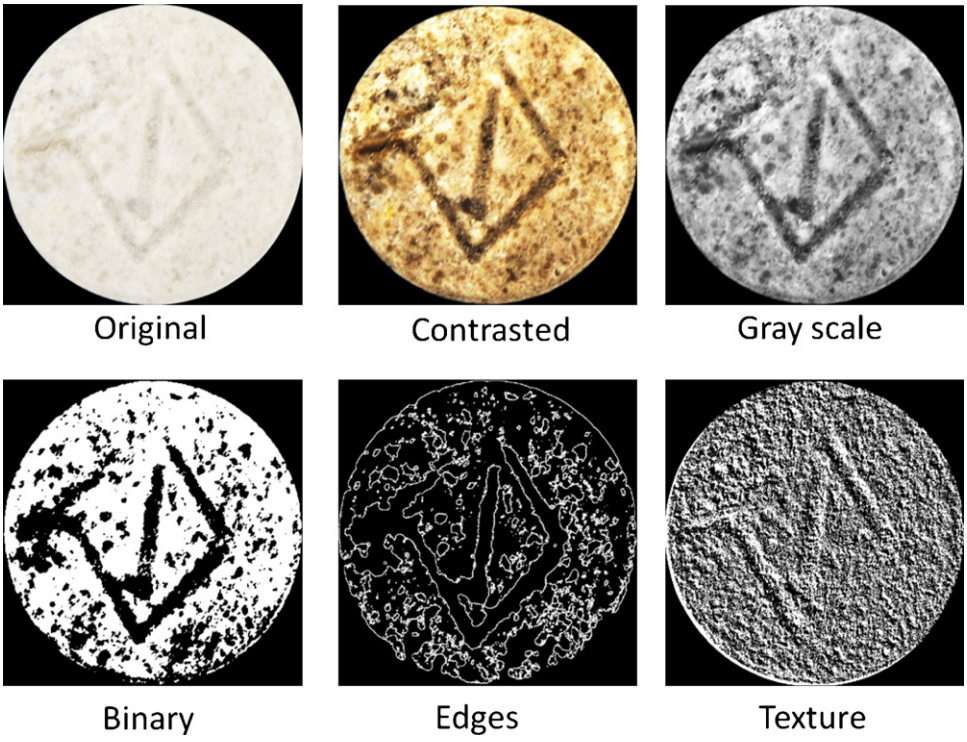

Fig. 2. Visual characteristics extracted of a pill.

[28]. An image is thus represented by a histogram that accounts for the amount of small patches present in it. The BoF method involves three steps: (1) feature detection and description, which consists of dividing the image into small patches, typically of 8×8 pixels. A local descriptor is computed to each patch; commonly descriptors such as the scale-invariant feature transform (SIFT) or the discrete cosine transform (DCT) coefficients. Here we chose to build a vector representation with 192 DCT coefficients for each patch by concatenating the first 64 DCT coefficients obtained for each RGB color channel; (2) codebook construction, which consists in clustering the resulting representation vectors in order to select a set of $k = 1000$ cluster centroids that are representative. Here, we used a k-means clustering algorithm and we obtained a 1000 words codebook; and finally (3) BoF representation, which consists at representing each image by a k-bin histogram by finding and counting for each patch the closest word in the codebook. An overview of the BoF process is illustrated in Fig. 3.

2.3. Pill visual similarity

2.3.1. Visual feature similarity

Given a particular visual feature, the similarity between two pill images can be obtained by comparing the corresponding histograms extracted from each image for the particular visual feature. There are different ways to compare histograms. In this work, we use a methods referred to as *histogram intersection* [29], which has been shown one of the best metrics to compare histograms in CBIR systems. The histogram intersection between two histograms is defined as,

$$K \cap (h_a, h_b) = \sum_{i=1}^{n} \min(k_a(i), k_b(i))$$

where h_a and h_b are for histograms a and b, and the min function retrieves the minimum value between the ith bin of both histograms. In other words, the function measures the amount of overlap of the two histograms; if both histograms are identical the overlap is maximum.

The resulting similarities between pills can be represented using a distance matrix, as illustrated in Fig. 4 for a set of 237 ecstasy pills. Each cell (pixel) represents the similarity between the ith pill and the jth pill. The whiter the intensity of the pixel, the higher the similarity between the corresponding pills.

2.3.2. Evaluation of the similarity measures

Evaluating different similarity measure is a difficult task. Some method might discriminate between groups of pills while other not, and vice versa. Therefore, statistical tools are required that enable a rigorous evaluation. The simplest analysis consists in representing graphically the distributions of similarity values obtained for both black (negative distribution) and white pixel (positive distribution) of the target matrix shown in Fig. 4 (right). A perfect method will lead to non overlapping distribution, that is, a threshold value can be chosen that unambiguously classify the intra-batch from the inter-batch similarity values.

A more sophisticated approach consists in reporting the rate at which true positive events occur versus the false positive rate. In that case, the perfect method is the one with a true positive rate of 1 and a false positive rate of 0. Again, this condition only occurs if a threshold value allows discriminating unambiguously inter- from intra-batch values. In real conditions, this analysis, referred to as ROC (Receiver Operating Characteristics) curves allows, indeed, to determine the threshold value that meets users' expectations, that is the best compromise between true and false positive rate.

Another possibility is to evaluate the impact of similarity in other tasks such as clustering. This impact can be analyzed measuring the entropy of the resulting groups of pills after the clustering process. A perfect clustering is that in which images of the same batch are clustered in the same group, that is to say, entropy measures the degree to which each cluster consists of pills of a single batch.

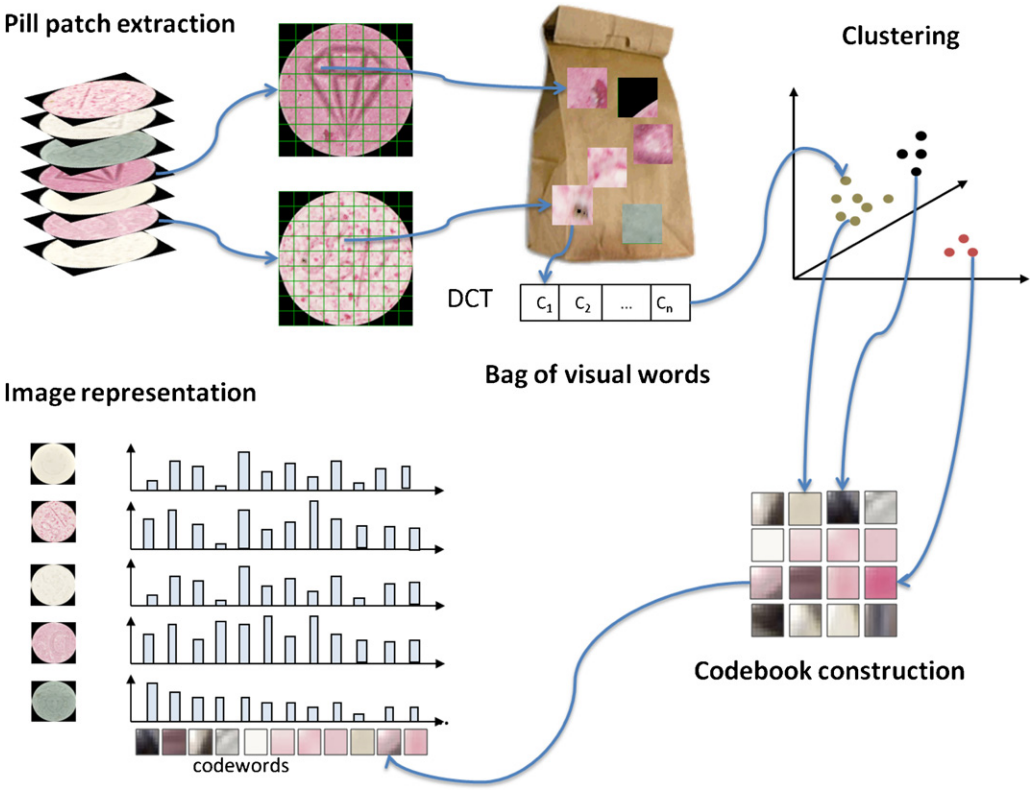

Fig. 3. Bag of features process to represent pill Ecstasy images.

2.3.3. Area overlap

The goal of the similarity learning task is to find a similarity measure of visual characteristics that assigns a high value to pills from the same production batch (in our case pills coming from a same seizure), while returning a small value indicates otherwise (pills coming from seizures knowing being unrelated by law enforcement information). Fig. 4 (right) shows the ideal similarity matrix or target matrix. This latter allows us to measure the discrimination power obtained with different visual features.

1. The power of discrimination (POD) for a given similarity function is evaluated as explained below:
2. The different intra-batch similarities are recorded in a 100-bins histogram, h_{inter}
3. Another histogram, h_{inter}, is built in a similar way as the first one, but this time sampling pairs of pills from different batches, i.e., inter-batch similarities.
4. Both histograms were normalized with L1-norm.
5. Both histograms are compared calculating the amount of overlap using histogram intersection: $K \cap (h_{inter}, h_{bintra})$. Fig. 5

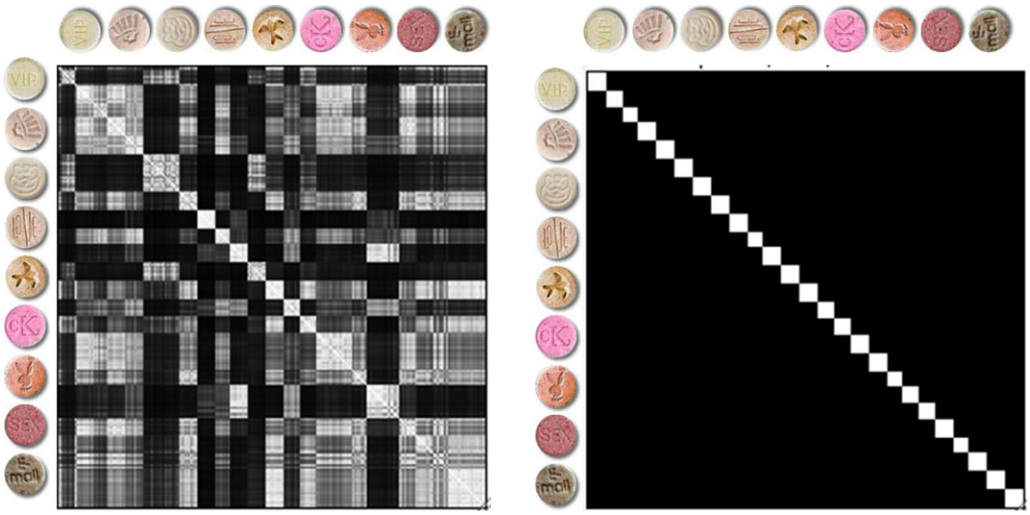

Fig. 4. Similarity matrix for a collection of 237 pills obtained using the histogram intersection of Gray visual feature (left). As an example, the ideal distance matrix obtained using a priori knowledge (right). (For interpretation of the references to color in this figure legend, the reader is referred to the web version of the article.)

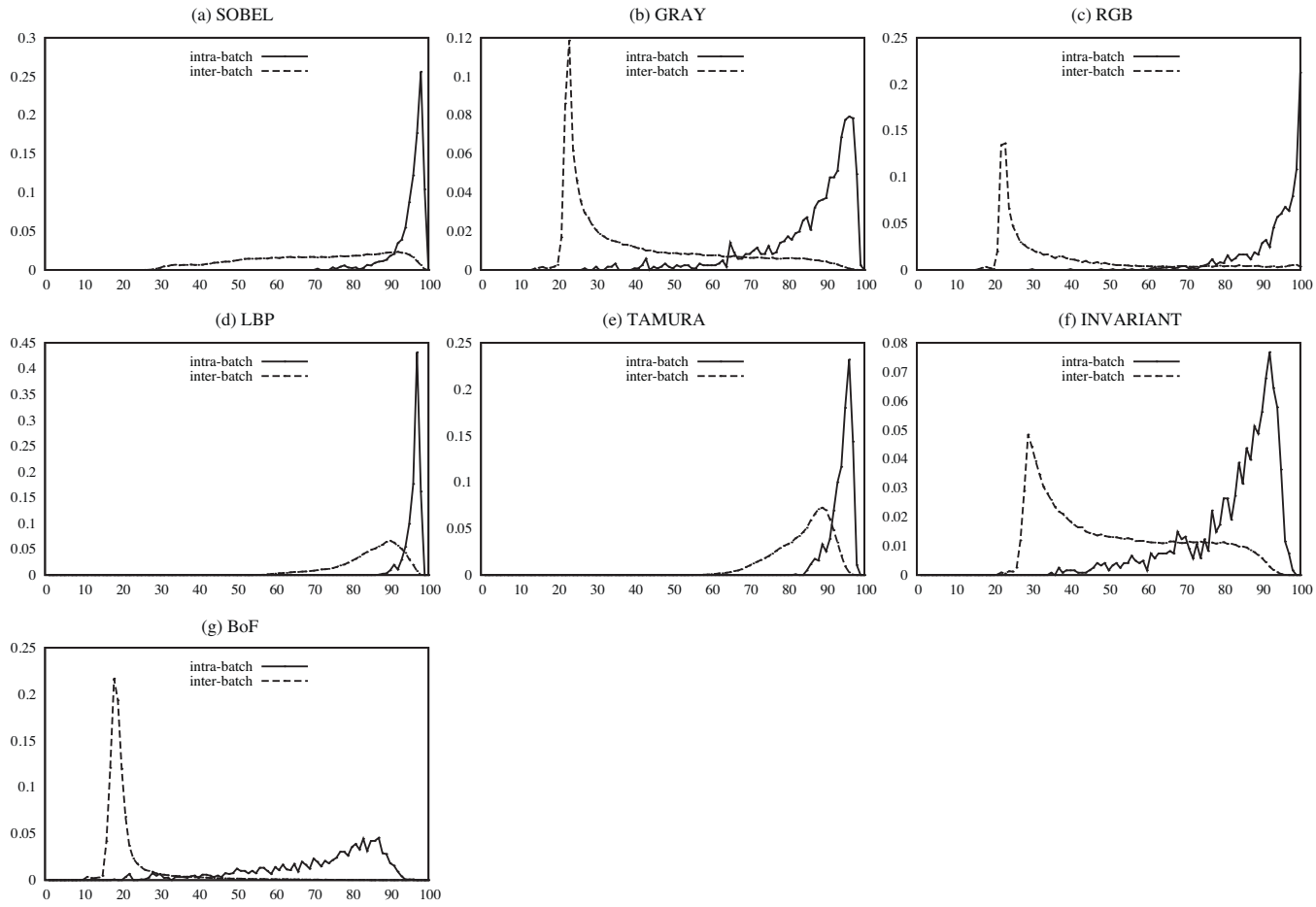

Fig. 5. Overlap between inter-batch and intra-batch distributions obtained using (a) sobel edge, (b) gray, (c) color, (d) invariant feature, (e) local binary patterns, (f) tamura texture and (g) bag of feature.

shows an illustration of h_{inter} and h_{intra} for a particular visual pill similarity function.

2.3.4. ROC analysis

To evaluate the ability of the particular visual similarity function to discriminate whether a pair of pills belong to the same batch or not, we used the area under the ROC (Receiver Operating Characteristics) curve [30]. In this context, a visual similarity function along with a given threshold is evaluated as a classifier as follows:

- True positive (tp): the pills belong to the same batch and their similarity is higher or equal than the threshold,
- True negative (tn): the pills belong to different batches and their similarity is lower or equal than the threshold,
- False positive (fp): the pills belong to the different batches and their similarity is higher or equal than the threshold.
- False negative (fn): the pills belong to the same batch and their similarity is higher than the threshold.

To construct the ROC curve, the threshold value is varied within a given interval, calculating the corresponding values for the sensitivity (true positive rate, TPR = $tp/(tp+fn)$) and specificity (false positive rate, FPR = $fn/(fp+tn)$), which are then plotted to form the ROC curve.

2.3.5. Entropy

We want to measure the impact of visual similarity functions in the construction of pill clusters. We used the entropy measure [31], which is a classification-oriented measure commonly used to validate cluster quality taking into account cluster labels – in our case, a priori, batch information. Entropy measures the degree to which each cluster consists of pills of a single batch. A cluster with high entropy has pills from different batches, a cluster with low entropy is more homogeneous, i.e., most of the pills belong to the same batch, thus, a lower entropy value is preferred. The entropy of a particular clustering is calculated as follows. For cluster j we compute P_{ij}, the probability that a pill of cluster i belongs to batch j as $P_{ij}=m_{ij}/m_i$, where m_i is the number of objects in cluster i and m_{ij} is the number of objects of pills of batch j in cluster i. Using this batch distribution, the entropy of each cluster i is calculated using $e_i = -\sum_{i=1}^{K}(m_i/m)\, e_i$, where K is the number of clusters and m is the total number of pills.

3. Results and discussions

In order to evaluate our strategy, we built a collection of 621 pictures of ecstasy pills consisting of 215 batches i.e. 187 batches of 2 pills, 2 batches of 3 pills, 1 batch of 4 pills, 4 batches of 8 pills, 5 batches of 9 pills and 16 batches of 10 pills. A second collection of images was prepared by resizing the original pictures to 256×256 pixels in order to accelerate the extraction process. All the functions were implemented using Java libraries, open source

packages such as ImageJ (http://rsbweb.nih.gov/ij/), Colt (http://acs.lbl.gov/software/colt/), LingPipe (http://alias-i.com/lingpipe/), the JavaScript InfoVis Toolkit (http://thejit.org), and other functions developed in our group. The experiments were performed using a standard desktop computer (Intel quad core with 4GB RAM) and were achieved in less than 130 s when the whole set was considered and image features were previously extracted.

3.1. Comparison of visual similarity functions

The POD for each visual similarity function was evaluated as described in Section 2.3.3. Pairs of pills belonging to the same batch were randomly selected and their similarity measured using a given similarity function. The results obtained for intra-batch distances (corresponding to the white pixels in Fig. 4 (right)) were represented by a histogram h_{intra}, while the resulting inter-batch distances (black pixels in Fig. 4 (right)) were represented by a histogram h_{inter} superimposing both histogram permits to visualize the POD. Indeed, overlapped histograms means poor POD, while well separated histograms means high POD. Example of such histograms is presented in Fig. 5, while Table 1 shows the obtained histogram intersection for each visual similarity function. Note that the BoF representation led to the lowest overlap, 10.59%, followed by RGB visual similarity function with 14.81%.

The POD for each visual similarity function was also evaluated using a ROC analysis, as discussed in Section 2.3.2. Table 1 shows both the area overlap and the area under the ROC curve (AUC).

Fig. 6 shows the ROC curve computed for each visual feature, and the column "Area under ROC curve" of Table 1 shows the corresponding area under the ROC curves [30]. With the exception of linear binary pattern and color, the visual similarity functions were ranked in the same order by both area overlap and AUC. The BoF visual similarity function was best ranked by the three proposed evaluation methods, that is, area overlap, ROC analysis, and clustering entropy. This result can be attributed to the capacity of BoF to find patterns that are characteristic from an image collection, which then constitute the codebook. Indeed, this approach was shown successful in other domains such as natural scene analysis, medical image annotation and content-based image retrieval [34]. It is important to notice that the BOF representation requires learning a visual codebook from the image collection and this implies an additional computation effort. However, this is compensated by the improved affectivity of the representation, which is reflected by the different performance measures.

3.2. Impact of visual similarity function in clustering

Cluster analysis is the task of assigning a set of objects into groups so that the objects in the same cluster are more similar to each other that to the ones in other clusters. Clustering is a common technique for statistical data analysis used for knowledge discovery. In this paper we used a hierarchical clustering algorithm

Table 1
Performance evaluation of each visual similarity function.

Visual feature	Area overlap	Area under ROC curve	Area under entropy curve
Bag of features	10.59%	0.987	327.843
Local binary pattern	17.72%	0.971	369.247
Tamura texture	26.51%	0.942	430.746
Gray	23.13%	0.951	433.599
Sobel edges	24.71%	0.949	475.048
Invariant feature	35.00%	0.907	499.384
Color (RGB)	14.81%	0.968	533.384

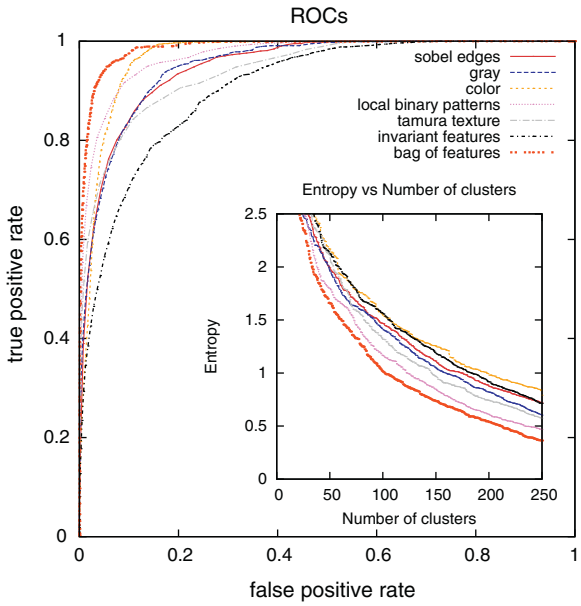

Fig. 6. ROC curves for each visual similarity functions. Insert: corresponding entropy curves.

called *single-linkage* to analyze relationships among ecstasy pills. Hierarchical clustering creates a hierarchy of clusters that can be represented by a tree structure called dendrogram. The algorithm starts by merging individual elements into clusters and progressively merges the resulting new clusters according to the distance between them. In our case, the similarity matrix is used as input to the algorithm since it reflects the distance (similarity) between pill images. Fig. 7 shows an example of a resulting dendrogram. For illustration purposes we superimposed the batch number inside 22 pills. Note that images of batches 2 and 3 are automatically organized in the same subtree, which allows revealing connections between tablets of different batches.

We also performed an objective evaluation of the impact of visual similarity functions in clustering using the entropy measure described in Section 2.3.3. We calculated the entropy varying the number of clusters, that is, we cut the dendrogram obtained for each visual similarity function and calculated its entropy. Fig. 6 shows a plot of the entropy versus the number of cluster. This plot was generated for ranges X: [5,250] clusters and Y: [0,2.5] entropy. The column "Area under entropy curve" in Table 1 shows the area under entropy curves for each visual feature. Note that BoF obtains the lowest value, which means that this feature is the best one for clustering as was described in Section 2.3.2.

3.3. Exploration of the image collection

The hierarchical structure of the obtained dendrogram allows organizing the image collection in a way that can be exploited to explore the relationships between tablets. We are interested in offering exploration tools that allow the user to visually navigate the image dataset. To reach this objective we developed a component based on the JavaScript InfoVis Toolkit,[1] which is an information visualization component that allows visualizing and exploring a hierarchy of objects. In this prototype (Fig. 8), we deployed the complete image dataset. The component uses a radial tree layout [32], in which the view is determined by the selection of a focus node. The algorithm used by the component is based on the radial layout method [33] by linearly interpolating the polar coordinates of the nodes and constraining the layout during interactions to keep it as similar as possible to the previous layout.

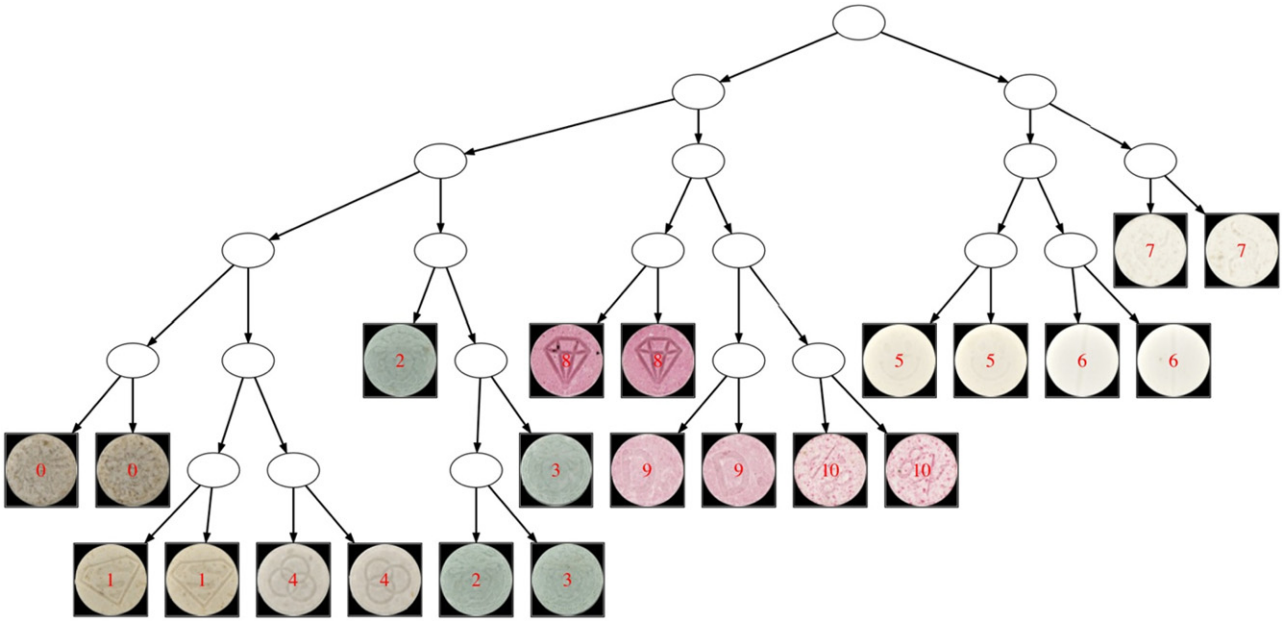

Fig. 7. Dendrogram generated by hierarchical clustering. Number inside indicates the corresponding batch membership.

However, when the number of images is large, it is necessary to display a summary of the collection, i.e., a subset of the collection that is representative and that can be used as starting point in the exploration process. In a future work we will address this issue by finding a representative image (centroid) to be displayed instead of all the members of the group.

Finally, an important aspect, of the profiling problem is the fact that images of different seizures can belong to the same production batch. Additional information (geo-location, infra-red spectra, etc.) can be used to build complementary visual similarity functions and combined with the existing information to achieve more accurate clustering, if necessary.

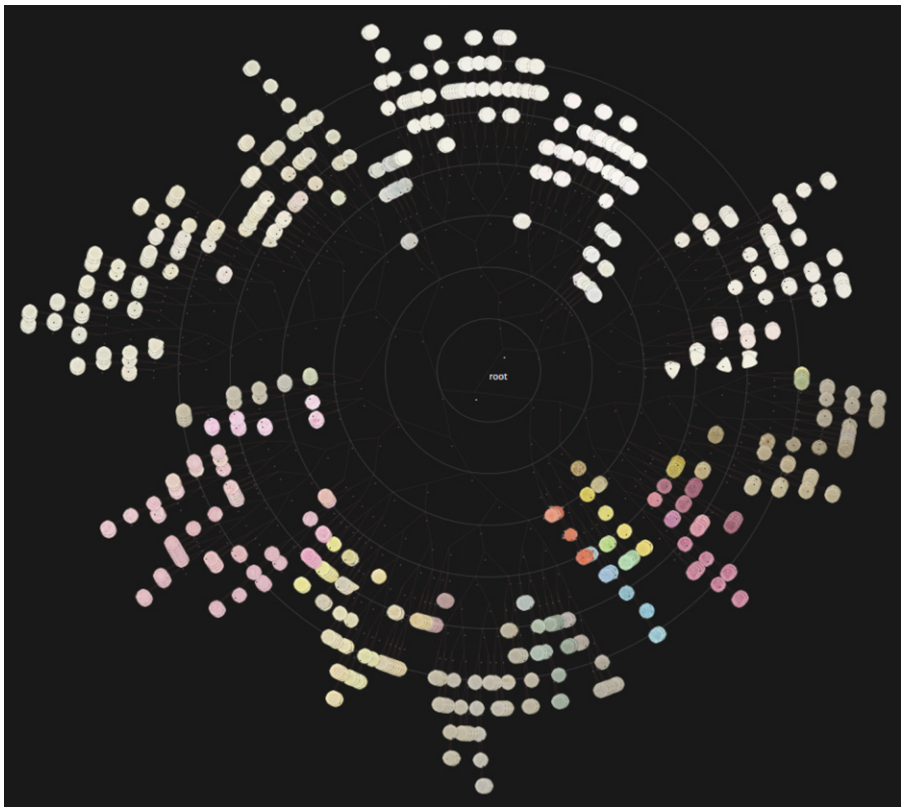

Fig. 8. Ecstasy pill explorer prototype. 621 pills are represented.

4. Conclusions

This paper presented a new approach for the profiling of illicit tablets using pictures of ecstasy pills. This powerful tool might help finding links between illicit drugs seizures by exploring the collection of image to decipher the structure of criminal organizations behind this traffic. The costs for its implementation are low in comparison with more sophisticated methods such as GC–MS and GC–IRMS, since it only relies on the visual characteristics of the pills. Interestingly, this little and easy to get information permits to efficiently group pills according to their seizures. As expected, the similarity function that allows extracting features that are characteristic of this data set performed better than the similarity functions based on standard features. In addition, supplementary information, such as IR spectra, can readily be included in our procedure, thereby allowing to refine the results if necessary.

We are currently working to include different kind of additional information such as seizure reports (date of seizure, place, active substances and cutting agent) and IR spectra to offer the users with the opportunity to select different levels of analysis according to their needs and to the availability of the data.

Acknowledgements

This work was partially funded by: the École Polytechnique de Lausanne, Institute of Chemical Sciences and Engineering; Université de Lausanne, Institut de Police Scientifique de Lausanne; The COLCIENCIAS project *Representation and Classification of Large Medical Image Collections*number 2020100114381; The COLCIENCIAS project *Sistema para la Recuperación de Imágenes Médicas utilizando Indexación Multimodal* number 202010017297.

References

[1] United Nations Office on Drugs and Crime, World Drug Report 2011, United Nations, New York, 2009.
[2] L. Aalberg, K. Andersson, C. Bertler, H. Boren, M.D. Cole, J. Dahlen, Y. Finnon, H. Huizer, K. Jalava, E. Kaa, E. Lock, A. Lopes, A. Poortman-van der Meer, E. Sippola, Development of a harmonised method for the profiling of amphetamines. I. Synthesis of standards and compilation of analytical data, Forensic Sci. Int. 149 (2–3) (2005) 219–229.
[3] L. Aalberg, K. Andersson, C. Bertler, M.D. Cole, Y. Finnon, H. Huizer, K. Jalava, E. Kaa, E. Lock, A. Lopes, A. Poortman-van der Meer, E. Sippola, J. Dahlen, Development of a harmonised method for the profiling of amphetamines. II. Stability of impurities in organic solvents, Forensic Sci. Int. 149 (2–3) (2005) 231–241.
[4] K. Andersson, K. Jalava, E. Lock, H. Huizer, E. Kaa, A. Lopes, A. Poortman-van der Meer, M.D. Cole, J. Dahlen, E. Sippola, Development of a harmonised method for the profiling of amphetamines. IV. Optimisation of sample preparation, Forensic Sci. Int. (2005).
[5] K. Andersson, E. Lock, K. Jalava, H. Huizer, S. Jonson, E. Kaa, A. Lopes, A. Poortman-van der Meer, E. Sippola, L. Dujourdy, J. Dahlen, Development of a harmonised method for the profiling of amphetamines. VI. Evaluation of methods for comparison of amphetamine, Forensic Sci. Int. 169 (1) (2007) 86–99.
[6] E. Lock, L. Aalberg, K. Andersson, J. Dahlen, M.D. Cole, Y. Finnon, H. Huizer, K. Jalava, E. Kaa, A. Lopes, A. Poortman-van der Meer, E. Sippola, Development of a harmonised method for the profiling of amphetamine. V. Determination of the variability of the optimised method, Forensic Sci. Int. (2005).
[7] M.M. van Deursen, E.R.A. Lock, A.J. Poortman-van der Meer, Organic impurity profiling of 3,4-methylenedioxymethamphetamine (MDMA) tablets seized in The Netherlands, Sci. Justice 46 (3) (2006) 135–152.
[8] K. Kuwayama, H. Inoue, J. Phorachata, K. Kongpatnitiroj, V. Puthaviriyakorn, K. Tsujikawa, H. Miyaguchi, T. Kanamori, Y.T. Iwata, N. Kamo, T. Kishi, Comparison and classification of methamphetamine seized in Japan and Thailand using gas chromatography with liquid–liquid extraction and solid-phase microextraction, Forensic Sci. Int. 175 (2–3) (2008) 85–92.
[9] H. Inoue, Y.T. Iwata, K. Kuwayama, Characterization and profiling of methamphetamine seizures, J. Health Sci. 54 (6) (2008) 615–622.
[10] Y.T. Iwata, K. Kuwayama, K. Tsujikawa, H. Miyaguchi, T. Kanamori, H. Inoue, Seized methamphetamine samples with unique profiles of stable nitrogen isotopic composition documented by stable isotope ratio mass spectrometry, Forensic Toxicol. 28 (2) (2010) 119–123.
[11] J. Lee, Y. Park, W. Yang, H. Chung, W. Choi, H. Inoue, K. Kuwayama, J. Park, Cross-examination of liquid–liquid extraction (LLE) and solid-phase microextraction (SPME) methods for impurity profiling of methamphetamine, Forensic Sci. Int. 215 (1–3) (2012) 175–178.
[12] K. Kuwayama, K. Tsujikawa, H. Miyaguchi, T. Kanamori, Y. Iwata, H. Inoue, S. Saitoh, T. Kishi, Identification of impurities and the statistical classification of methamphetamine using headspace solid phase microextraction and gas chromatography–mass spectrometry, Forensic Sci. Int. 160 (1) (2006) 44–52.
[13] F. Bonadio, P. Margot, O. Delémont, P. Esseiva, Headspace solid-phase microextraction (HS-SPME) and liquid–liquid extraction (LLE): comparison of the performance in classification of ecstasy tablets (Part 2), Forensic Sci. Int. 182 (1–3) (2008) 52–56.
[14] F. Bonadio, P. Margot, O. Delémont, P. Esseiva, Optimization of HS-SPME/GC–MS analysis and its use in the profiling of illicit ecstasy tablets (Part 1), Forensic Sci. Int. 187 (1–3) (2009) 73–80.
[15] H.A.S. Buchanan, N.N. Daeid, W. Meier-Augenstein, H.F. Kemp, W.J. Kerr, M. Middleditch, Emerging use of isotope ratio mass spectrometry as a tool for discrimination of 3,4-methylenedioxymethamphetamine by synthetic route, Anal. Chem. 80 (9) (2008) 3350–3356.
[16] H.A.S. Buchanan, W.J. Kerr, W. Meier-Augenstein, N.N. Daeid, Organic impurities, stable isotopes, or both: a comparison of instrumental and pattern recognition techniques for the profiling of 3,4-methylenedioxymethamphetamine, Anal. Meth. 3 (10) (2011) 2279–2288.
[17] R. Marquis, C. Weyermann, C. Delaporte, P. Esseiva, L. Aalberg, F. Besacier, J.S. Bozenko Jr., R. Dahlenburg, C. Kopper, F. Zrcek, Drug intelligence based on MDMA tablets data. 2. Physical characteristics profiling, Forensic Sci. Int. 178 (1) (2008) 34–39.
[18] Z. Geradts, J. Bijhold, Content based information retrieval in forensic image databases, J. Forensic Sci. 47 (2) (2002) 285–292.
[19] Y.B. Lee, U. Park, A.K. Jain, S.W. Lee, Pill-ID: Matching and retrieval of drug pill images, Pattern Recogn. Lett. (2011).
[20] D. Kim, J. Chun, Drug Image Retrieval by Shape and Color Similarity of the Medication, in: First ACIS/JNU International Conference on Computers, Networks, Systems and Industrial Engineering (CNSI), Jeju Island, (2011), pp. 387–390.
[21] M. Lopatka, M. Vallat, Surface granularity as a discriminating feature of illicit tablets, Forensic Sci. Int. 210 (1–3) (2011) 188–194.
[22] L.M. Given, S. Ruecker, H. Simpson, E. Sadler, A. Ruskin, Inclusive interface design for seniors: image-browsing for a health information context, J. Am. Soc. Inform. Sci. Technol. 58 (11) (2007) 1610–1617.
[23] S. Siggelkow, H. Burkhardt, Improvement of Histogram-Based Image Retrieval and Classification, in: 16th International Conference on Pattern Recognition, vol. 16, Quebec, Canada, (2002), pp. 367–370.
[24] A.P. Berman, L.G. Shapiro, Flexible image database system for content-based retrieval, Comp. Vis. Image Und. 75 (1) (1999) 175–195.
[25] I. Sobel, Neighborhood coding of ninary images for fast contour following and general following binary processing, Comp. Graphics Image Process. 8 (1) (1978) 127–135.
[26] T. Deselaers, D. Keysers, H. Ney, Features for Image Retrieval: A Quantitative Comparison, in: 26th DAGM Symposium Pattern Recognition, vol. 3175, Tübingen, Germany, (2004), pp. 228–236.
[27] L. Fei-Fei, P. Perona, A Bayesian Hierarchical Model for Learning Natural Scene Categories, in: IEEE Computer Society Conference on Computer Vision and Pattern Recognition, vol. II, San Diego, USA, (2005), pp. 524–531.
[28] I. Biederman, Recognition-by-components: a theory of human image understanding, Psychol. Rev. 94 (2) (1987) 115–147.
[29] A. Barla, F. Odone, A. Verri, Histogram Intersection Kernel for Image Classification, in: International Conference on Image Processing, vol. 3, Barcelona, Spain, (2003), pp. 513–516.
[30] T. Fawcett, An introduction to ROC analysis, Pattern Recogn. Lett. 27 (8) (2006) 861–874.
[31] D. Tan, D. Taniar, K.A. Smith, A clustering algorithm based on an estimated distribution model, Int. J. Bus. Intel. Data Mining 1 (2) (2005) 229–245.
[32] K.P. Yee, D. Fisher, R. Dhamija, M. Hearst, Animated Exploration of Dynamic Graphs with Radial Layout, in: Proceedings of the IEEE Symposium on Information Visualization, San Diego, USA, (2001), pp. 43–50.
[33] G. Di Battista, P. Eades, R. Tamassia, I.G. Tollis, Graph Drawing: Algorithms for the Visualization of Graphs, Prentice Hall, Upper Saddle River, NJ, 1999.
[34] A. Cruz-Roa, J.C. Caicedo, F.A. González, Visual pattern mining in histology image collections using bag of features, Artif. Intell. Med. 52 (2) (2011) 91–106.

[1] http://thejit.org/.